Role of induced quadrupoles in the simulation of intrinsic point defects in AgCl and NaCl

Radha D. Banhatti and Y. V. G. S. Murti
Department of Physics, Indian Institute of Technology, Madras, India 600036
(Received 17 February 1993; revised manuscript received 7 May 1993)

The paper presents a detailed formulation of the energetics of point defects in ionic crystals that takes into account the quadrupolar deformation of the ions surrounding the defect within a polarizable-point-ion picture. The dipolar polarizabilities are modeled to represent correctly the static dielectric response of the crystal. Consideration of the axial symmetry of the electric-field-gradient tensor, the residual site symmetries in the defect crystal, and the symmetry of the quadrupolar-polarizability tensor leads to a cylindrical symmetry for the induced quadrupoles for both the vacancy and interstitial type of defects. These quadrupoles give rise to an additional polarization contribution to the defect formation besides affecting the dipolar energy. Computer codes have been developed based on this model and results are presented for vacancies and interstitials in AgCl and NaCl and discussed in detail. The calculations use a two-body central-force potential with well-represented van der Waals interactions. It is found that there is a substantial contribution from the quadrupoles to the defect enthalpy. The investigations reveal the comparative importance of accurate modeling of the polarization features *vis à vis* subtle refinements in the interionic potential.

I. INTRODUCTION

Silver chloride has rocksalt structure and has many features in common with sodium chloride. Yet, one of the main distinguishing features is that the charge and mass transport in AgCl proceeds via the cation-interstitial or interstitialcy mechanism,[1] unlike in NaCl where the vacancy mechanism dominates. Experiments have demonstrated that AgCl has predominant cationic Frenkel defects, while in NaCl the Schottky defects are the dominant species. A large body of data from conductivity and diffusion experiments has quantified the Frenkel defect formation enthalpy (h_F) in AgCl (Ref. 2) to be ~ 1.45 eV and the Schottky formation enthalpy (h_S) in NaCl (Refs. 3 and 4) to be 2.3–2.5 eV. The anion diffusion experiments in AgCl indicate an appreciable concentration of Schottky defects with an inferred value[2] of $h_S \approx 1.7$–2.0 eV, but there is no experimental information on h_F in NaCl.

An isolated point defect, since it is charged, causes extensive lattice deformation in the form of distortion of electronic shells and ion relaxations. If these have to be simulated satisfactorily then one needs (a) a polarization model that is physically sound for correctly estimating the effect of the long-ranged electrostatic field due to the defect and (b) an interionic potential that gives a reasonable representation of the short-range repulsive and dispersion forces that come into play. The criteria for testing the success of such a simulation are the following: (1) its estimate of the point defect formation enthalpies is in good agreement with experiments; (2) it is able to predict the dominant defect species, with the same polarization and potential model for different defect environments; and (3) the equilibrium relaxations of ions tally with the features of the interionic potential and yield a stable defect configuration.

The earliest theoretical simulation[5] to estimate h_S and h_F was based on the polarizable-point-ion (PPI) model. This model due to Mott and Littleton (ML) represented the polarized lattice as a collection of point dipoles. Since the model led to a very large value for the static dielectric constant (ϵ_s) and hence overestimated the contribution of polarization to defect formation it was abandoned in spite of its elegant physical formulation.

The shell model[6] and the deformation dipole model[7] which were originally developed for the lattice dynamics of perfect crystals accounted for the reduction in polarization due to short-range forces. Of these two, the shell model is more widely used in defect calculations. Though this was successful it brought in some unwanted features. Firstly, in the shell model, the potential parameters of the salt considered are coupled to other model parameters, and the focus shifted heavily to the modeling of interionic potential. Also, these parameters are obtained by extensive fitting to the bulk crystal (elastic and dielectric) properties. The success or failure of estimation of the defect formation enthalpies then was attributed to the finer details of the functional form and relative strengths of the potential terms. Secondly, the shell model brings in artifacts which complicate the calculation and render extension to higher-order multipole deformations difficult. The limitations of the shell-model calculations are especially noticeable in the estimation of h_S and h_F in AgCl (Ref. 8) as compared to NaCl.

An alternative approach to defect simulations in ionic crystals that proved successful in the alkali-halide family is the modified polarizable-point-ion (MPPI) model.[9] This retains the simplicity of the PPI model and reproduces ϵ_s by *redefining* the electronic polarizabilities as suitable to the static lattice deformations. The main assertion of the model is that once ϵ_s is correctly simulated, the defect calculations are not very sensitive to subtle

changes of the potential.

It has long been realized that the long-ranged field of the defect cannot be adequately simulated within the limits of a dipole approximation. In fact, it has been pointed out[10] that some of the unphysical results obtained in the shell model stem mainly from ignoring the effects of induced quadrupole (and higher) moments. However, in view of the fact that it would require quite a few additional parameters to explicitly include quadrupole moments, there has been only occasional lip service paid to the subject.

It is the purpose of this paper to show that the simple but physically sound MPPI model paves the way for extending the ML scheme to include the effect of field gradients around the defect and the resulting induced quadrupoles. We call this the extended polarizable-point-ion model (EPPI).[11] We present the detailed formulation of this model and incorporate the symmetry properties of the various defect environments under consideration and show that in the cases of AgCl and NaCl the defect formation enthalpies are estimated correctly. Especially, in the case of AgCl, be it the vacancy or the interstitial, it turns out that the contribution of the quadrupoles to the polarization energy cannot be ignored.

The structure of the paper is as follows. Section II presents in brief the scheme used for defect calculations. Section III presents in detail the salient features of the various polarization models, in order to highlight the crucial aspects of the EPPI model. Sections IV and V discuss the vacancy and interstitial environments, respectively, based on the symmetry properties associated with their nearest-neighbor lattice sites. Detailed formulae of the various fields at the site of interest are written down explicitly. In Sec. VI a brief account of the potential model is given along with a tabulation of the potential parameters used. Section VII describes the energy terms and the computer code developed. Section VIII presents the results along with a discussion on the emerging trends, to be followed by Sec. IX with conclusions.

II. SCHEME OF CALCULATION

Treating the lattice as a dielectric continuum, Jost[12] recognized the fact that, as an ion is removed from a lattice site, the vacant site bearing an effective charge induces dipoles. The potential of these dipoles makes a gainful contribution to the defect energy:

$$W_p = -\frac{e^2}{2R}\left[1-\frac{1}{\epsilon_s}\right], \tag{1}$$

where R is the radius of the cavity around the vacancy. This considerably underestimates the energy of formation of a defect as it neglects the lattice relaxations and the consequent changes in the short- and long-range interactions. The scheme developed by Mott and Littleton[5] divides the crystal into two regions, 1 and 2, where the second region is treated as a dielectric continuum. Region 1 consists of the defect and a few shells of ions around it. The polarization $\mathbf{P}$ at $\mathbf{r}$ in region 2 is given by

$$\mathbf{P} = \frac{(\epsilon_s - 1) q_d \mathbf{r}}{4\pi\epsilon_s |\mathbf{r}|^3}, \tag{2}$$

where q_d is charge of the defect. Mott and Littleton then proceeded to apportion the dipole moments to the two sublattices in proportion to the respective polarizabilities in each primitive cell of volume v_m. The dipole moments are given by

$$\gamma_{c,a} = \left[\frac{\alpha_{c,a}+\alpha_d}{\alpha_c+\alpha_a+2\alpha_d}\right] v_m \mathbf{P}. \tag{3}$$

The displacement of an ion i of charge q_i in region 2 is given by

$$\gamma_{d,i} = \left[\frac{\alpha_d}{\alpha_c+\alpha_a+2\alpha_d}\right] \frac{v_m}{q_i} \mathbf{P}, \tag{4}$$

where $\alpha_{c,a}$ represents the electronic polarizability of the cation or the anion and α_d represents the displacement polarizability.

The contribution of ions of region 1 to the energy of the lattice with defect is treated on an atomistic basis with the displacements and induced dipole moments evaluated explicitly by applying the force balance method.

For treating defects which are electrical singularities, it is this method which we have used with refinements; namely, using the energy minimization method to evaluate the defect formation energy. Following Norgett,[13] we may write the total energy of the defect lattice as

$$E_D = E_1(\boldsymbol{\beta}) + E_2(\boldsymbol{\beta},\boldsymbol{\gamma}) + E_3(\boldsymbol{\gamma}), \tag{5}$$

where $E_1(\boldsymbol{\beta})$ is the energy of region 1 and $\boldsymbol{\beta}$ represents both the displacements and induced dipole moments of region 1, $E_3(\boldsymbol{\gamma})$ is the energy of region 2, and $E_2(\boldsymbol{\beta},\boldsymbol{\gamma})$ is the interaction energy between the two regions. Assuming harmonic approximation for region 2 and supposing the equilibrium displacements and dipole moments $\boldsymbol{\gamma}_0$ of region 2 to be known via the ML approximation as given by Eqs. (3) and (4), results in

$$E_D = E_1(\boldsymbol{\beta}) + E_2(\boldsymbol{\beta},\boldsymbol{\gamma}_0) - \left.\frac{\partial E_2}{\partial \boldsymbol{\gamma}}\right|_{\boldsymbol{\gamma}_0} \cdot \boldsymbol{\gamma}_0. \tag{6}$$

The equilibrium relaxations are found from $\partial E_D/\partial\boldsymbol{\beta}=0$. In our calculation, the dipole moments and the relevant induced quadrupole-moment components are functions of the relaxations of the ions of region 1. This reduces the number of independent variables in the calculation as elaborated in Secs. IV and V.

III. POLARIZATION MODELS

In this section we review briefly the various models for the estimation of polarization energy in the presence of a defect in order to highlight and present our MPPI and EPPI models in perspective.

A. Previous models

The effects of the internal long-ranged field generated by a charged defect is treated within the point dipole ap-

proximation. The optical polarizabilities of the ions were calculated by Tessmann *et al.*[14] (TKS polarizabilities) from the Lorentz-Lorenz relation

$$\frac{\epsilon_\infty - 1}{\epsilon_\infty + 2} = \frac{4\pi}{3v_m}(\alpha_c + \alpha_a) , \tag{7}$$

where ϵ_∞ is the high-frequency dielectric constant. Then, the electronic dipole moments $\mathbf{p}_{c,a}$ are given by

$$\mathbf{p}_{c,a} = \alpha_{c,a}\mathbf{F} , \tag{8}$$

where $\mathbf{F}$ is the total field due to the monopoles of region 1 and dipoles of regions 1 and 2. The corresponding polarization energy is

$$W_p = -\tfrac{1}{2}\mathbf{p}\cdot\mathbf{F}_1^m , \tag{9}$$

where $\mathbf{F}_1^m$ is the field of monopoles of region 1. This is the polarizable-point-ion (PPI) model. The displacement polarizability α_d deduced from the short-range interactions between nearest neighbors is given by

$$\alpha_d = e^2/k , \tag{10a}$$

where k is the force constant given by (for the rocksalt structure)

$$k = 4\left[\phi_{ij}''(r_0) + \frac{2}{r_0}\phi_{ij}'(r_0)\right] . \tag{10b}$$

ϕ'' and ϕ' are the second and first derivatives of the short-range potential ϕ and r_0 is the nearest cation-anion separation. When the values of α_c, α_a, and α_d so obtained are substituted in the Clausius-Mossotti equation

$$\frac{\epsilon_s - 1}{\epsilon_s + 2} = \frac{4\pi}{3v_m}(\alpha_c + \alpha_a + 2\alpha_d) , \tag{11}$$

the value of ϵ_s turns out to be large. This implies that, in the continuum limit, W_p will be even more overestimated than that given by Jost. This drawback of the PPI model arises from the fact that it does not take into account the reduction of polarization due to the overlap of the neighboring ions.

To include the effect of short-range forces on polarization, it was proposed by Szigeti[15] that the ions behave as if they carried an effective charge that was smaller than the full electronic charge. The effective charge e^* is obtained from ϵ_s, ϵ_∞, the characteristic optical frequency ω_0 of the crystal, and the reduced mass M of the two ions, using the relation

$$\epsilon_s - \epsilon_\infty = \frac{4\pi N(Ze^*)^2}{9M\omega_0^2}(\epsilon_\infty + 2)^2 . \tag{12}$$

This gives rise to an additional "deformation dipole moment" proportional to $(e^* - e)x$, where x is the displacement. This is the deformation dipole model. This deformation dipole is to be treated as a dynamic property, and the cohesion of ionic crystals is still to be understood on the Born model[16] in terms of an array of point charges of magnitude $\pm e$. These dipoles are located on the anions in the estimation of the dynamical properties of the perfect crystal. However, in the case of defects, where both the ions are treated as polarizable and deformable, it is not very clear how to place the deformation dipoles. Furthermore it is assumed that the deformation polarization is not directly coupled to any field-induced polarization on the ion that may also be present.[7]

The shell model[17] is yet another model used to account for the short-range polarization. This is a mechanical model, where each ion consists of a massive core and a negatively charged shell of electrons attached to the core by a harmonic and isotropic spring. The total charge of the core plus the shell is equal to $\pm Ze$, the ion charge. The short-range forces are generally taken to act between shells only, since these forces arise primarily from the overlap and exchange interactions between outer electrons which are represented as shells in this model. Two spring constants are needed for each ion. The shell model fits the potential and shell parameters to perfect crystal properties and to both ϵ_s and ϵ_∞, so that W_p is estimated correctly. The success of the model is seen from its application to determine point defect formation enthalpies in numerous systems.

The shell model, however, has the following serious limitations. Firstly, it has twice the number of variables as compared to the PPI model; this makes it computationally cumbersome. Secondly, in the process of fitting of crystal properties to the potential, it sometimes yields unphysical values to the shell parameters—such as a positive charge for the shell. Thirdly, being a parametric model, it offers very little scope for representing the electronic states of the system. Fourthly, extension to higher-order multipoles involves introducing further artifacts.

In view of these considerations it is desirable to have a fresh approach to the polarization aspect of the defect calculation.

B. Modified polarizable-point-ion (MPPI) model

In a calculation which involves many parameters it is essential to identify the more important quantities. If these chosen quantities are fitted to or reproduced, then it is a matter of detail to show that the results are not very sensitive to the other parameters. The point defect in an ionic crystal, whether it is a Schottky or Frenkel defect, is an electrical singularity rather than an elastic defect. In recognition of this and the fact that the defect calculations focus on those parameters which are relevant even in the absence of an external field, the one most relevant quantity is the static dielectric constant ϵ_s. Since the shortcoming of the PPI model is in the overestimation of ϵ_s and ignoring the effect of short-range interactions on the polarization, it was rectified as follows: retaining the estimation of α_d from short-range interactions as given by Eq. (10), the effect of reduction of polarization due to the overlap of ions is absorbed in $\alpha_c + \alpha_a$, so as to reproduce the experimental ϵ_s. This is the modified polarizable-point-ion (MPPI) model.[9] It has been shown that the way the two polarizabilities are apportioned is not so critical, but a plausible way is to take

$$\frac{\alpha_c}{\alpha_a}=\left[\frac{r_c}{r_a}\right]^3 , \tag{13}$$

where r_c and r_a are the Pauling ionic radii.

Thus the MPPI model *renormalizes* the electronic polarizabilities as suited to the static environment, and they are naturally different from the TKS polarizabilities. The advantages of the model are as follows: firstly, the point dipole model with all its elegance and ease of formulation is retained. Secondly, the effect of short-range forces on polarization is taken care of without introducing any artifacts, since redefined α_c and α_a simply indicate that in a crystal environment the electronic response to a static field is limited by overlap. Thirdly and *most* importantly, it has put to rest the debate and the ensuing computational complications as to how large the size of region 1 should be. It has been demonstrated that within the MPPI model the values of the defect formation enthalpies are *independent* of the size of region 1. As a result of this, region 1 is *always* chosen to be the defect and its nearest neighbors. This model has been used successfully in various defect environments.[18]

C. Extended polarizable-point-ion (EPPI) model

As the defect field is predominantly electrostatic and hence long ranged, there exist significant electric field gradients whose contribution to the polarization energy cannot be ignored without a detailed investigation. Spurred on by the success of the MPPI dipolar model, we have developed a formalism to extend it to include the effect of induced quadrupoles.

In this model region 1 contains the defect and its nearest neighbors whose displacements, induced dipole and quadrupole moments, are to be evaluated explicitly. The second region, however, is treated within the dipole approximation as in the ML scheme.

The quadrupole moment is a second-rank, symmetric traceless tensor, and has six independent components in general. Its components Q_{ij} are given by

$$Q_{ij}=\alpha^q_{ijkl}F_{kl} , \tag{14}$$

where α^q_{ijkl} is the quadrupole polarizability and F_{kl} is the kl component of the electric field gradient tensor; in all first-principles calculations in the free-ion environment, α^q_{ijkl} is treated as spherically symmetric and is represented as a scalar quantity (α^q).[19] However, in the crystal environment the quadrupolar polarizability tensor components have the following relations:[20]

$$\begin{aligned}&\alpha^q_{1111}=\alpha^q_{2222}=\alpha^q_{3333}=\tfrac{2}{3}\alpha^q ,\\ &\alpha^q_{1212}=\alpha^q_{2323}=\alpha^q_{3131}=\tfrac{1}{2}\alpha^q ,\\ &\alpha^q_{1122}=\alpha^q_{2233}=\alpha^q_{3311}=-\tfrac{1}{3}\alpha^q .\end{aligned} \tag{15a}$$

All the other components are zero. The full O_h symmetry of the crystal is destroyed by the presence of the defect. The nearest neighbors of a vacancy and interstitial have C_{4v} and C_{3v} site symmetry, respectively. The principal axes of the field gradient tensor in the case of the vacancy are oriented along [100], [010], and [001]. In the case of the interstitial, one of the principal axes (z') is along $\langle 111\rangle$ and the other two (x',y') lie in the $\{111\}$ plane. In such a principal axis system, we have

$$\sum F_{kl}=0 \quad \text{for } k\neq l , \tag{15b}$$

where the summation extends over the entire crystal. In general if the relaxations of the ions are taken to be radial to the defect, then it follows that

$$\sum F_{x'x'}=\sum F_{y'y'}=-\tfrac{1}{2}\sum F_{z'z'} , \tag{15c}$$

where z' is taken along the symmetry axis in the radial direction of the field point. With these symmetry properties of the crystal, the electric field gradient tensor and the quadrupole polarizability tensor, it turns out that the induced quadrupoles have a cylindrical symmetry.

This simplifies the formulation considerably since there is only one independent component, say $Q_{z'z'}$, which needs to be determined, and the quadrupole tensor components are related by

$$\begin{aligned}&Q_{x'x'}=Q_{y'y'}=-\tfrac{1}{2}Q_{z'z'} ,\\ &Q_{x'y'}=Q_{x'z'}=Q_{y'z'}=0 .\end{aligned} \tag{15d}$$

In view of the presence of quadrupoles in the first region, the electrostatic part of the defect energy should take into account all interactions among quadrupoles, dipoles, and monopoles. The equation for the induced dipole moment has an extra term: namely, the quadrupole field. The induced dipole and quadrupole moments need to be solved for simultaneously. The equations for one of the nearest-neighbor ions with the symmetric axis along z' are superscripts 1 and 2 over F (field) and W (energy) indicate regions 1 and 2, respectively.

$$p^{c,a}_{z'}=\alpha_{c,a}\{\mathbf{F}^1_m+\mathbf{F}^1_d+\mathbf{F}^2_d+\mathbf{F}^1_q\}_{z'} , \tag{16}$$

$$Q^{c,a}_{z'z'}=\alpha^q_{c,a}\frac{\partial}{\partial z'}\{\mathbf{F}^1_m+\mathbf{F}^1_d+\mathbf{F}^2_d+\mathbf{F}^1_q\}_{z'} , \tag{17}$$

where $\mathbf{F}^1_m$ is the field due to monopoles, including the real and virtual charges of region 1. $\mathbf{F}^1_d+\mathbf{F}^2_d$ is the field due to dipoles in regions 1 and 2, and $\mathbf{F}^1_q$ is the field due to quadrupoles of the first region. In the next section we consider explicitly the fields in the vacancy and interstitial environments.

IV. VACANCY DEFECT

When an ion from a normal lattice position is missing, we have a vacancy defect. As we are dealing with thermal defects, we can treat these as isolated point defects with a very low defect concentration and neglect effects of defect-defect interaction.

Region 1 then consists of the vacancy, say an anion vacancy, and its six nearest neighbors. It is customary to perform all calculations with the defect as the origin. The defect has a virtual positive charge $+e$. Since the crystal has cubic symmetry, the effect of removing an ion produces radial displacements in the ions. The principal axes (x',y',z') of the quadrupole-moment tensor coincide with the x, y, and z axes along the [100], [010], and [001] directions [see Fig. 1(a)]. The first-region cations being

equivalent, we consider a representative ion A [Fig. 1(a)] at $(0,0,1)r_0$ and set up the simultaneous equations for the dipole moment p_z and quadrupole component Q_{zz}.

The cation at $(0,0,1)r_0$ relaxes to a displaced position $(0,0,1+s_c)r_0$, where s_c is the fractional displacement of the region-1 ions in the respective radial directions. The various fields acting at the displaced sites are given by

$$F^I_{m,z}=\frac{e}{(1+s_c)^2 r_0^2}+\frac{e}{r_0^2}\left[\frac{1.6642}{(1+s_c)^2}-\frac{1}{(2+s_c)^2}-\frac{4(1+s_c)}{\{(1+s_c)^2+1\}^{3/2}}\right], \tag{18}$$

where the radial component of the monopole field estimated includes the contribution from the real charges of the cations of region 1 at the displaced sites and from the virtual charges of the vacated sites and the vacancy.

The radial component of the field due to region-1 dipoles is

$$F^I_{d,z}=-\frac{2.3713 p_c}{r_0^3(1+s_c)^3}, \tag{19}$$

where p_c is the magnitude of the induced dipole moment.

The field due to region-2 dipoles is estimated using a separate program to evaluate the lattice summation over 34 shells of ions around the defect. The field at the desired $(0,0,1+s_c)r_0$ site is evaluated for a mesh of relaxations (s_c). It is then smoothly fitted to a fourth-degree polynomial in s_c and the field is written as

$$F^2_{d,z}=\frac{e}{r_0^2}[\text{odds}(s_c)M_c+\text{evens}(s_c)M_a], \tag{20}$$

where odds(s_c) represents the contribution to the field from those ions (l_1,l_2,l_3) whose sum $(l_1+l_2+l_3)$ is odd (cations), and evens(s_c) from those ions with $(l_1+l_2+l_3)$ even (anions). The polynomials are

$$\begin{aligned}\text{evens}(s_c)&=-4.7166s_c^4+14.8716s_c^3+9.2984s_c^2\\&\quad-2.1459s_c-1.9659,\\ \text{odds}(s_c)&=-1.056s_c^4+0.2219s_c^3+0.1847s_c^2\\&\quad-0.6753s_c-0.3888.\end{aligned} \tag{21}$$

M_c and M_a, the apportioning parameters for the polarization contribution of the cations and anions respectively, are defined as

$$M_{c,a}=\left[\frac{\alpha_{c,a}+\alpha_d}{\alpha_c+\alpha_a+2\alpha_d}\right]\frac{\epsilon_s-1}{2\pi\epsilon_s}. \tag{22}$$

The source ion quadrupole moments can be assigned by using Eqs. (14) and (15). The potential at the field point $\mathbf{r}_f=(1+s_c)r_0\hat{\mathbf{k}}$ due to the induced quadrupole Q_p on a cation located at the position $\mathbf{r}_p$ ($\neq\mathbf{r}_f$) is

$$\phi_q=\frac{1}{2}\left[\frac{Q_{p,xx}(x_f-x_p)^2+Q_{p,yy}(y_f-y_p)^2+Q_{p,zz}(z_f-z_p)^2}{|\mathbf{r}_f-\mathbf{r}_p|^5}\right]. \tag{23}$$

The field due to quadrupoles is then obtained from $-\nabla\phi_q$. Since the relaxations of the ions are radial to the defect, all the fields are also radial at the field point. This means that

$$F^1_{q,z}=-Q_{p,zz}\frac{z_{fp}}{|\mathbf{r}_{fp}|^5}+\frac{5}{2}\frac{z_{fp}}{|\mathbf{r}_{fp}|^7}(Q_{p,xx}x_{fp}^2+Q_{p,yy}y_{fp}^2+Q_{p,zz}z_{fp}^2), \tag{24}$$

where z_{fp} is a short notation for z_f-z_p and $\mathbf{r}_{fp}=\mathbf{r}_f-\mathbf{r}_p$. The sum over the first region cations yields[21]

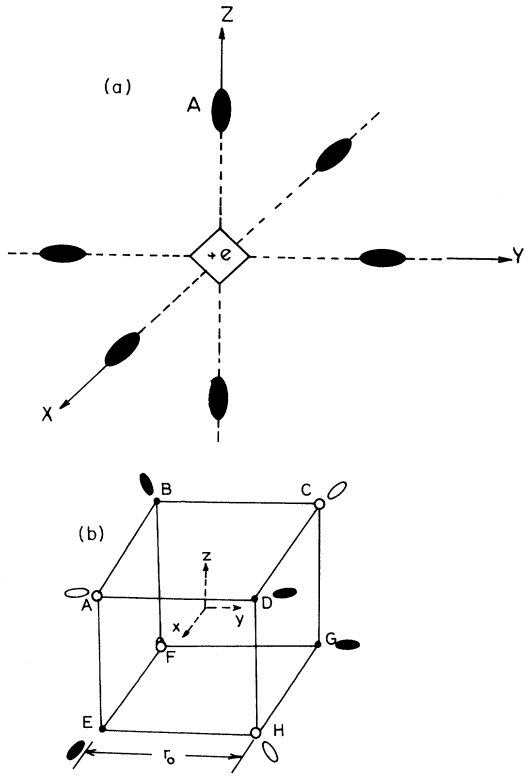

FIG. 1. (a) Anion vacancy defect, region 1. Solid ellipses depict the quadrupolar deformation of the cations in their displaced sites. (b) Cation interstitial defect, region 1. Solid circles represent cations at their normal lattice sites; open circles represent anions at their normal lattice sites; quadrupolar deformations are depicted for these ions in their displaced sites by ellipses.

$$F^1_{q,z}=\frac{0.8893Q^c}{(1+s_c)^4r_0^4} \ . \tag{25}$$

where $Q^{c,a}=Q^{c,a}_{z,z}$. Using the expressions for the fields, one has for the z component of the dipole moment at $(0,0,1+s_c)r_0$

$$p_z^c\equiv p_c=\alpha_c\left[\frac{e}{(1+s_c)^2r_0^2}+\frac{e}{r_0^2}\left[\frac{1.6642}{(1+s_c)^2}-\frac{1}{(2+s_c)^2}-\frac{4(1+s_c)}{\{(1+s_c)^2+1\}^{1.5}}\right]-\frac{2.3713p_c}{(1+s_c)^3r_0^3}+\frac{e}{r_0^2}[\text{odds}(s_c)M_c+\text{evens}(s_c)M_a]+\frac{0.8893}{(1+s_c)^4r_0^4}Q^c\right] \ . \tag{26}$$

In order to determine the quadrupole moment, we need the zz component of field gradients:

$$F^1_{m,zz}=\frac{q_p}{|\mathbf{r}_{fp}|^5}[|\mathbf{r}_{fp}|^2-3z_{fp}^2] \ . \tag{27}$$

At the field point being considered, the sum of contributions to this gradient due to all monopoles of region 1 amounts to

$$F^1_{m,zz}=\frac{2e}{(2+s_c)^3r_0^3}+\frac{4e\{2(1+s_c)^2-1\}}{\{(1+s_c)^2+1\}^{2.5}r_0^3}-\frac{2.9571e}{(1+s_c)^3r_0^3} \ . \tag{28}$$

The field gradient at the point $\mathbf{r}_f$ due to a dipole $\mathbf{p}$ located at $\mathbf{r}_p$ is given by

$$F^1_{d,zz}=\frac{3(\mathbf{p}\cdot\mathbf{r}_{fp})}{|\mathbf{r}_{fp}|^7}[|\mathbf{r}_{fp}|^2-5(z_{fp})^2]+\frac{6pz_p(z_{fp})}{|\mathbf{r}_p||\mathbf{r}_{fp}|^5} \ . \tag{29}$$

Such contributions to the gradient from all the dipoles of region 1 add up to

$$F^1_{d,zz}=\frac{3.5570}{(1+s_c)^4r_0^4}p_c \ . \tag{30}$$

We have evaluated the field gradient of the dipoles situated in region 2 by differentiating the polynomials odds(s_c) and evens(s_c) with respect to the relaxation s_c. We have checked that such a derivative is a good estimate of the dipole gradient sums by explicit calculation. This also follows from the smooth nature of the dipole field polynomials. Then the field gradient can be written as

$$F^2_{d,zz}=\frac{e}{r_0^3}[\text{odds}'(s_c)M_c+\text{evens}'(s_c)M_a] \ , \tag{31}$$

where the odds$'(s_c)$ and evens$'(s_c)$ are the corresponding derivatives with respect to s_c.

The zz component of the quadrupole we are interested in is easily obtained by finding the derivative of the z component of the quadrupole field as given by Eq. (25) with respect to z_f. Using the source ion quadrupole moments Q_p, we obtain the field gradient at the $(0,0,1+s_c)r_0$ ion site due to other first-region cations as[21]

$$F^1_{q,zz}=-\frac{2.7066}{(1+s_c)^5r_0^5}Q^c \ . \tag{32}$$

Collecting all these terms together, the induced quadrupole moment of the cation in the displaced position is

$$Q^c_{zz}\equiv Q^c=\alpha_c^q\left[\frac{2e}{(2+s_c)r_0^3}+\frac{4\{2(1+s_c)^2-1\}e}{\{(1+s_c)^2+1\}^{2.5}r_0^3}-\frac{2.9571e}{(1+s_c)^3r_0^3}+\frac{3.5570p_c}{(1+s_c)^4r_0^4}+\frac{e}{r_0^3}[\text{odds}'(s_c)M_c+\text{evens}'(s_c)M_a]-\frac{2.7066Q^c}{(1+s_c)^5r_0^5}\right] \ . \tag{33}$$

Using the simultaneous equations (26) and (33), the induced dipole moments and quadrupole moments are determined as functions of the displacements (s_c).

The associated electronic polarization energy, which is a major contribution to the removal of an ion from the lattice, is given by

$$W^1_{p,e}=-3p_z^cF^1_m \ . \tag{34}$$

The quadrupolar polarization energy is given by

$$W^1_q=6\left[(\tfrac{1}{2})(-\tfrac{1}{6})\sum_{ij}Q_{ij}F^1_{m,ij}\right] \ , \tag{35}$$

where 6 indicates the fact it includes contributions from all ions of region 1. The factor $\frac{1}{2}$ arises from the induced nature of the quadrupoles. Since the monopoles are the only permanent moments, only their fields and gradients need to be considered in evaluating the dipole and quadrupole polarization energies. Using the symmetry properties of the field gradient tensor together with the cylindrical symmetry of the quadrupole moments from Eqs. (14) and (15), we get

$$W^1_q=-\tfrac{3}{4}Q^c_{zz}F^1_{m,zz} \ . \tag{36}$$

This gives the additional contribution to the vacancy formation energy arising from quadrupole interactions.

It is straightforward to set up the equations for the cation vacancy. The region-1 ions other than the defect are anions, and the charge of the defect and the region-1 ions is $-e$. The fractional relaxation of the anions is s_a. By inspection, the terms corresponding to monopole, dipole, and quadrupole fields and field gradients due to other region-1 ions can be written. Since the vacancy here is cationic, the odd shells are anions and the even shells are cations. The region-2 dipole sum is then written as a sum of the odds$(s_a)M_a$ and evens$(s_a)M_c$, where the polynomials odds(s_a) and evens(s_a) are as in Eq. (21) except that they are functions of s_a. The equations then are set up for p_z^a and Q_{zz}^a and solved. The expressions for the energies remain unchanged.

V. INTERSTITIAL DEFECT

Consider an interstitial defect. Here we have a cation residing in an interstitial site chosen as the origin. Its nearest neighbors are four cations and four anions located at $(\pm\frac{1}{2},\pm\frac{1}{2},\pm\frac{1}{2})r_0$ at the corners of cube of side r_0 [Fig. 1(b)]. The fractional relaxations of the cations are s_c and those of the anions are s_a.

Region 1 then consists of these eight ions and the defect. Each of these eight ions are located at sites of C_{3v} symmetry and experience only radial displacement and fields. The dipole moment vector is then given by $p_{c,a}(\pm\hat{\mathbf{i}},\pm\hat{\mathbf{j}},\pm\hat{\mathbf{k}})$.

However, the quadrupole tensor components Q_{ij}s along the x, y, and z axes are not cylindrically symmetric. It turns out that the field gradient components (F_{ij}) have the following relations:

$$\sum F_{xx}=\sum F_{yy}=\sum F_{zz}=0\ ,$$
$$\sum F_{yz}=\sum F_{zx}=\sum F_{xy}\ , \tag{37}$$

where the sum is over the entire crystal. This yields one independent quadrupole moment component $Q_{xy}^{c,a}$. We need to relate this component with the principal value $(Q_{z'z'}^{c})$ of the Q tensor. It is a standard result that in a system with a symmetry axis (here, all $\langle 111\rangle$ directions) the principal axes are (1) the symmetry axis itself and (2) any two axes in a plane normal to the symmetry axis. Such a transformation yields not only a diagonal quadrupole tensor but one in which it is cylindrically symmetric. For example, for the cation at $0.5(\hat{\mathbf{i}},\hat{\mathbf{j}},\hat{\mathbf{k}})r_0$ the principal axes are $[1\ -1\ 0]$, $[1\ 1\ -2]$, and $[1\ 1\ 1]$. The transformation matrix from the principal axes to the x, y, and z axes $\langle 100\rangle$ gives

$$Q_{xy}^{c,a}=\tfrac{1}{2}Q^{c,a}\ . \tag{38a}$$

where $Q^{c,a}=Q_{z'z'}^{c,a}$. As the coordinates of all ions are expressed in terms of the x, y, and z axes, the formulation and calculation is carried out more easily in this coordinate system. From Eqs. (15) it then turns out that

$$Q_{xy}^{c,a}=\alpha_{c,a}^{q}F_{xy}\ . \tag{38b}$$

Two representative ions [D and F in Fig. 1(b)] are chosen in region 1 to evaluate p_c, p_a, Q^c, and Q^a. They are, respectively, a cation at $\{\frac{1}{2}+s_c/\sqrt{3}\}(\hat{\mathbf{i}},\hat{\mathbf{j}},\hat{\mathbf{k}})r_0$ and an anion at $-\{\frac{1}{2}+s_a/\sqrt{3}\}(\hat{\mathbf{i}},\hat{\mathbf{j}},\hat{\mathbf{k}})r_0$. Four linear simultaneous equations need to be set up.

We proceed to write now as in the vacancy case the various fields for the cation at $\mathbf{r}_f=(0.5+s_c/\sqrt{3})(\hat{\mathbf{i}},\hat{\mathbf{j}},\hat{\mathbf{k}})r_0$.

The contribution of the eight real charges at the displaced position, the eight virtual charges at the lattice sites, and the real charge at the defect site to the monopole field is found to be radial and is given by

$$F_{m,c}^{1}r_0^2=\left[\frac{e}{3a^2}+\frac{\sqrt{3}e(1+\sqrt{3}s_c)}{\{\frac{2}{3}s_c^2+a^2\}^{1.5}}-\frac{\sqrt{3}e(2+\sqrt{3}s_c)}{\{(s_c^2/3)+2a^2\}^{1.5}}-\frac{e}{3b^2}-\frac{\sqrt{3}e\left[1+\dfrac{3s_c-s_a}{\sqrt{3}}\right]}{\{b^2+2c^2\}^{1.5}}+\frac{3e}{\sqrt{6}(2a-1)^2}+\frac{e}{3(a-0.5)^2}\right]\ , \tag{39}$$

where

$$a=1+\frac{s_c}{\sqrt{3}},\quad b=1+\frac{s_c+s_a}{\sqrt{3}},\quad \text{and } c=\frac{s_c-s_a}{\sqrt{3}}\ . \tag{39a}$$

The field due to region-1 dipoles is radial and is given by

$$F_{d,c}^{1}r_0^3=\left[\frac{p_a\left[2(s_c^2+s_a^2)-\dfrac{28s_cs_a}{3}-8\left\{\dfrac{s_c+s_a}{\sqrt{3}}\right\}-4\right]}{(b^2+2c^2)^{2.5}}-\frac{2p_a}{3^{1.5}b^3}-\frac{5p_c}{2^{1.5}(2a-1)^3}\right]\ . \tag{40}$$

The field of region-2 dipoles is radial to the defect, and the contribution from each dipole is distance dependent as in the vacancy case. The only difference is that now each shell of ions has an equal number of cations and anions. Hence an ion i with coordinates (l_1,l_2,l_3) contributes to evens(s_c) if $\{(l_1-\frac{1}{2})+(l_2-\frac{1}{2})+(l_3-\frac{1}{2})\}$ is even; otherwise it contributes to odds(s_c).

$$F^2_{d,c}=[\text{evens}(s_c)M_c+\text{odds}(s_c)M_a]e/r_0^2 , \tag{41}$$

where M_c and M_a are given by Eq. (22) and the dipole sums are

$$\begin{aligned}\text{evens}(s_c)&=-1.4751s_c^4+1.1585s_c^3+0.9170s_c^2-0.8455s_c-0.5916 ,\\ \text{odds}(s_c)&=2.3128s_c^4-6.0473s_c^3-5.4066s_c^2-1.3039s_c+0.1224 .\end{aligned} \tag{42}$$

The field of the region-1 quadrupoles is estimated using the general expression for the quadrupole field in the Cartesian x, y, and z axes. Making use of Eq. (38),

$$F^1_{q,c}\cdot r_0^4=\sqrt{3}\left\{Q^a\left[\frac{1}{6\sqrt{3}b^4}+\frac{2b^3-11bc^2-10b^2c+10c^3}{2(b^2+2c^2)^{3.5}}\right]+\frac{5Q^c}{2^{3.5}(2a-1)^4}\right\} . \tag{43}$$

The equation for p_c is then given by

$$p_c=\alpha_c[F^1_{m,c}+F^1_{d,c}+F^2_{d,c}+F^1_{q,c}] , \tag{44}$$

where the explicit expressions for the fields are given in Eqs. (39)–(43).

It is straightforward now to write by inspection the various expressions for the fields at the anion site at $\mathbf{r}_f=-(0.5+s_a/\sqrt{3})(\hat{\mathbf{i}},\hat{\mathbf{j}},\hat{\mathbf{k}})r_0$.

$$\begin{aligned}F^1_{m,a}r_0^2=&\left[-\frac{e}{3k^2}-\frac{\sqrt{3}e(1+\sqrt{3}s_a)}{\{\frac{2}{3}s_a^2+k^2\}^{1.5}}+\frac{\sqrt{3}e(2+\sqrt{3}s_a)}{\{(s_a^2/3)+2k^2\}^{1.5}}+\frac{e}{3m^2}\right.\\&\left.+\frac{\sqrt{3}e\left[1+\frac{3s_a-s_c}{\sqrt{3}}\right]}{\{m^2+2n^2\}^{1.5}}-\frac{3e}{\sqrt{6}(2k-1)^2}+\frac{e}{3(k-0.5)^2}\right]\end{aligned} \tag{45}$$

where

$$k=1+\frac{s_a}{\sqrt{3}},\quad m=1+\frac{s_a+s_c}{\sqrt{3}},\quad \text{and } n=\frac{s_a-s_c}{\sqrt{3}} . \tag{45a}$$

The dipole field due to region-1 ions at the anion site is given by

$$F^1_{d,a}r_0^3=\left\{\frac{p_c\left[2(s_c^2+s_a^2)-\frac{28s_cs_a}{3}-8\left\{\frac{s_c+s_a}{\sqrt{3}}\right\}-4\right]}{(m^2+2n^2)^{2.5}}-\frac{2p_c}{3^{1.5}m^3}-\frac{5p_a}{2^{1.5}(2k-1)^3}\right\} . \tag{46}$$

The field due to region-2 dipoles is evaluated as before and is

$$F^2_{d,a}=[\text{evens}(s_a)M_a+\text{odds}(s_a)M_c]e/r_0^2 , \tag{47}$$

where the dipole sums odds(s_a) and evens(s_a) are given by Eq. (42) with s_c replaced by s_a.

The field due to quadrupoles at the anion site is given by

$$F^1_{q,a}\cdot r_0^4=\sqrt{3}\left\{Q^c\left[\frac{1}{6\sqrt{3}m^4}+\frac{2m^3-11mn^2-10m^2n+10n^3}{2(m^2+2n^2)^{3.5}}\right]+\frac{5Q^a}{2^{3.5}(2k-1)^4}\right\} . \tag{48}$$

The equation for the magnitude of the anion dipole moment, p_a is then given by,

$$p_a=\alpha_a[F^1_{m,a}+F^1_{d,a}+F^2_{d,a}+F^1_{q,a}] , \tag{49}$$

where the explicit expressions for the fields are given in Eqs. (45)–(48).

In order to set up the equations for Q^c and Q^a we need to find only the field gradient component F_{xy} [see Eqs. (37) and (38)] at the two chosen sites D and F [Fig. 1(b)]. The monopole field gradient at the cation field site is

$$\begin{aligned}F^{1,c}_{m,xy}=&\left\{-\frac{e}{3^{1.5}a^3}-\frac{3e(s_c^2+2s_c/\sqrt{3})}{\{\frac{2}{3}s_c^2+a^2\}^{2.5}}+\frac{3e(1+s_c^2+4s_c/\sqrt{3})}{\{(s_c^2/3)+2a^2\}^{2.5}}+\frac{e}{3^{1.5}b^3}\right.\\&\left.+\frac{3ec(2+\sqrt{3}s_c+s_a/\sqrt{3})}{\{b^2+2c^2\}^{2.5}}-\frac{3e}{2^{2.5}(2a-1)^3}-\frac{e}{3^{1.5}(a-0.5)^3}\right\}\frac{1}{r_0^3} .\end{aligned} \tag{50}$$

The total field gradient due to the dipoles of region 1, at the cation site is

$$F^{1,c}_{d,xy}r_0^4=\left[\frac{p_a\{(2s_c+2s_a)+2\sqrt{3}\}}{(b^2+2c^2)^{2.5}}+\frac{p_a}{3b^4}+\frac{15p_c}{2^{2.5}\sqrt{3}(2a-1)^4}+\frac{15p_a[(1+\sqrt{3}s_a-s_c/\sqrt{3})(s_c^2-s_a^2/3-2s_cs_a/3+2c)]}{(b^2+2c^2)^{3.5}}\right] . \tag{51}$$

We have evaluated the field gradient of the dipoles situated in region 2 by differentiating the polynomials odds(s_c) and evens(s_c) given in Eq. (42) with respect to the relaxation s_c:

$$F^{2,c}_{d,xy}=\frac{e}{2r_0^3}[\text{odds}'(s_c)M_a+\text{evens}'(s_c)M_c] . \tag{52}$$

The expression for the sum of the field gradient of quadrupoles of region 1 is given by

$$F^{1,c}_{q,xy}r_0^5=\left\{Q^a\left[-\frac{1}{3^{1.5}b^5}+\frac{-9b^4-51c^4+114b^2c^2}{2(b^2+2c^2)^{4.5}}\right]-\frac{51Q^c}{2^{5.5}(2a-1)^5}\right\} . \tag{53}$$

It follows from Eqs. (38a) and (38b) that

$$Q^c=2Q^c_{xy}=2\alpha_c^q\frac{\partial}{\partial y}\{\mathbf{F}^1_{m,c}+\mathbf{F}^1_{d,c}+\mathbf{F}^2_{d,c}+\mathbf{F}^1_{q,c}\}_x , \tag{54}$$

where the field gradients are given in Eqs. (50)–(53).

The field gradients at the anion site $(-0.5-s_a/\sqrt{3})(1,1,1)r_0$ are obtained as follows. Replacing e with $-e$, and a, b, and c with k, m, and n, respectively [given by Eq. (45a)], and interchanging s_c and s_a in Eq. (50), we get the monopole field gradient. In addition to these substitutions, interchanging p_c and p_a in Eq. (51) gives the field gradient of dipoles of region 1 at the anion site. The field gradient due to dipoles of region 2 is

$$F^{2,a}_{d,xy}=\frac{e}{2r_0^3}[\text{odds}'(s_a)M_c+\text{evens}'(s_a)M_a] , \tag{55}$$

where the odds(s_a) and evens(s_a) given by Eq. (42) with s_a replacing s_c, and differentiated with respect to s_a. The field gradient of quadrupoles at the region-1 anion site has the same form as Eq. (53) except that Q^c and Q^a are interchanged and a, b, and c are replaced by k, m, and n, given in Eq. (45a). Thus the quadrupole component Q^a is found by setting up an equation of the same form as Eq. (54). That is,

$$Q^a=2Q^a_{xy}=2\alpha_a^q\frac{\partial}{\partial y}\{\mathbf{F}^1_{m,a}+\mathbf{F}^1_{d,a}+\mathbf{F}^2_{d,a}+\mathbf{F}^1_{q,a}\}_x . \tag{56}$$

The electronic dipole polarization energy is then given by

$$W^1_{p,e}=-0.5(4p_cF^1_{m,c}+4p_aF^1_{m,a}) , \tag{57}$$

where the monopole fields $F^1_{m,c}$ at the cation and $F^1_{m,a}$ at the anion site are radial to the defect.

In the x, y, and z coordinate axes system, the quadrupole contribution of the region-1 ions to the polarization energy is

$$W^1_q=-4\times\tfrac{1}{6}\times3(Q^c_{xy}\cdot F^{1,c}_{m,xy}+Q^a_{xy}\cdot F^{1,a}_{m,xy}) . \tag{58}$$

Using the symmetry relations given in Eqs. (15) and (38), we get

$$W^1_q=-(Q^c\cdot F^{1,c}_{m,xy}+Q^a\cdot F^{1,a}_{m,xy}) , \tag{59}$$

where p_c, p_a, Q^c, and Q^a are determined from the coupled set of simultaneous Eqs. (44), (49), (54), and (56).

VI. POTENTIAL MODEL

Since ionic crystals consist of closed-shell ions, it has been, in general, found adequate to invoke central force interionic potentials to model the contribution to the bulk properties of the overlap repulsion and dispersion forces. The short-range potential for a pair of ions of type i and j at separation r_{ij} is taken to be of the form

$$\phi^{sr}_{ij}=A_{ij}\exp[-r_{ij}/\rho_{ij}]-\frac{C_{ij}}{r_{ij}^6} , \tag{60}$$

where the A_{ij}'s are the preexponential constants for the overlap repulsion potential with the hardness parameters ρ_{ij}. The C_{ij}'s are the constants for the dipole-dipole van der Waals (vdW) interactions.

It is customary to determine the A_{ij}'s and the ρ_{ij}'s for a family of crystals by fitting[16] extensively to the bulk lattice properties, such as the cohesive energy, the bulk modulus, and equilibrium lattice constant. The van der Waals coefficients are then obtained from optical data or from some simplified theoretical estimates.

However, we have retained a simplified picture of the overlap repulsion, assuming it to be not significantly different from a molecular environment. Hence, we have adopted for the A_{ij}'s and ρ_{ij}'s the values from electron gas calculations[22] available in the literature for NaCl (Ref. 23) and AgCl.[24] These are given in Table I.

The larger cohesive energy of the AgCl salt (9.3–9.5 eV) compared to that of the NaCl salt (8.02 eV), in spite of nearly equal values for the interionic distance r_0 (2.75

TABLE I. Short-range overlap repulsion parameters.

Salt	A_{cc} (eV)	A_{ca} (eV)	A_{aa} (eV)	ρ_{cc} (Å)	ρ_{ca} (Å)	ρ_{aa} (Å)
NaCl	45 720.0	1736.30	1227.2	0.142	0.305	0.321
AgCl	16 528.0	2518.80	1227.2	0.237	0.327	0.321

TABLE II. vdW coefficients, polarizabilities, and ionic radii.

Salt	C_{ca} (eV Å^6)	C_{cc} (eV Å^6)	C_{aa} (eV Å^6)	α_c (Å^3)	α_a (Å^3)	α_d (Å^3)	r_c (Å)	r_a (Å)
AgCl	154.001	178.800	267.062	1.153	3.417	1.405	1.26	1.81
NaCl	5.571	6.169	18.905	0.143	1.032	2.607	0.95	1.81

and 2.82 Å), in both the cases and stronger repulsion in AgCl (see Table I) clearly points to a much stronger van der Waals interaction[25] than has been deduced from experiments or *ab initio* calculations. Our earlier investigations[26] confirm this. The potential model used for the present calculation is the same as set III of our previous work.[26] The van der Waals coefficient C_{ca} was obtained by fitting to the equilibrium lattice condition and C_{cc} and C_{aa} were obtained using the relations, based on London's formula,

$$\frac{C_{cc}}{C_{ca}}=\frac{\alpha_c(E_c+E_a)}{2\alpha_a E_a} \quad \text{and} \quad \frac{C_{aa}}{C_{ca}}=\frac{\alpha_a(E_c+E_a)}{2\alpha_c E_c}\ , \tag{61}$$

where E_c and E_a are the second excitation energies of the alkali ion[27] and electronegativity of the anion, respectively.[28] An aspect worth discussing is the effectiveness of a central force model, especially for AgCl, which exhibits a strong Cauchy violation. Other works that incorporate three-body interactions show that the contribution of this to the cohesive energy is of the order of a few percent.[25,29] Since the symmetry of either a vacancy or an interstitial is such that it leads only to radial displacements of the ions, we expect an explicit inclusion of either a triple-dipole model or a bond-bending model[30] would not significantly influence the defect formation process. As long as the relative strengths of the short-range attractive and repulsive forces are estimated in right proportion, the defect calculation may be insensitive to the finer refinements in the potential.

In the MPPI model the strength of $(\alpha_c+\alpha_a)$ is determined by α_d and ϵ_s. Estimation of α_d depends on the short-range parameters: A_{ca}, ρ_{ca}, and C_{ca}. Thus it turns out that the polarization energy contribution and the short-range parameters of the potential are interlinked in our approach of simulating the defect formation enthalpies. The vdW coefficients and the polarizabilities are given in Table II. The static dielectric constant is taken from the work of Lowndes and Martin.[31]

As pointed out earlier, the polarizabilities are redefined to be consistent with the static dielectric response of the crystal. Thus, they give a measure of how much the electronic polarizabilities of the ions are restricted in their static crystal environment due to short-range forces as compared to their free-ion values or even the TKS values, which correspond to the optical response of the crystal and where the overlap effects are of lesser significance. In this sense, due to the strongly contrasting properties of the short-range potentials of NaCl and AgCl—viz., strong van der Waals interactions, compactness of the Ag^+ ion, r_0 being smaller than what the additivity of ionic radii would imply—the polarizabilities of both the ions in AgCl are much larger than in NaCl. Further, the valence electron distribution of Cl^- in AgCl is expected to be expanded compared to the free-ion case (rather than shrunk as in alkali halides) in accordance with the observation[32] in AgBr. It thus follows that the electronic polarizabilities cannot be considered to be characteristic of the ions, but are strongly crystal dependent, being the outcome of an interplay of electronic deformations and short-range forces. It is therefore not surprising that α_a varies widely from NaCl to AgCl (Table II).

In order to study the effect of the quadrupole polarizability (α^q) of the anion or cation we have considered four cases.

Case 1. Here the calculation is carried out by setting the α^q's to zero. This gives an idea as to how much the dipole moment and dipole polarization energy are altered when one includes quadrupoles.

Case 2. Here we have used Mahan's value for α^q of the Ag^+ ion, which is based on a self-consistent field method and a modified Sternheimer's equation for polarizability within the local-density approximation. Mahan[33] estimated α^q for the Ag^+ ion to be 2.62 Å^5. A subsequent calculation by Mahan[34] for the alkali halides in the crystal environment yielded α^q for Cl^- ions between 5.00 and 7.00 Å^5 with the corresponding values for the cations Na^+, K^+, and Rb^+ in the range 0.06 to 1.43 Å^5. As α_d of Cl^- in AgCl falls in the range of α_d in RbCl and KCl, we take α^q of the Cl^- ion in AgCl to be 6.5 Å^5.

Case 3. Schmidt *et al.*[35] have estimated α^q for various ions using a coupled Hartree-Fock method in conjunction with the Watson sphere model to obtain the quantity of interest in the crystal environment. Self-consistency is incorporated by a method adapted from diagrammatic

TABLE III. Cation vacancy—various energy contributions; α^q=0.0 Å^5. (All energy terms in units of eV.)

Salt	s_a(min)	RLE	Coul.	Rep.	vdW	W_p^1	W_p^2	W_{cv}
AgCl	−0.005	8.85	0.16	−0.14	0.06	−1.68	−1.84	5.41
NaCl	0.080	8.02	−2.06	1.01	−0.04	−0.06	−1.70	5.20
NaCl[a]	0.080	7.95	−2.06	1.08	−0.05	0.05	−1.73	5.23

[a]Potential parameters from the Fumi-Tosi model (Ref. 16).

TABLE IV. Anion vacancy—various energy contributions; $\alpha^q=0.0$ Å^5. (All energy terms in units of eV.)

Salt	s_c(min)	RLE	Coul	Rep	vdW	W_p^1	W_p^2	W_{av}
AgCl	0.040	9.15	−1.15	1.27	−0.57	−0.28	−2.08	6.33
NaCl	0.090	8.00	−2.27	1.22	−0.05	0.21	−1.79	5.29
NaCl[a]	0.090	8.10	−2.27	1.21	−0.06	0.18	−1.77	5.37

[a]Potential parameters from the Fumi-Tosi model (Ref. 16).

many-electron perturbation theory. α^q's for Na^+, Ag^+, and Cl^- are 0.063, 1.44, and 5.53 Å^5, respectively.

Case 4. Schmidt *et al.*[35] have also estimated α^q in free ions but with self-consistency effects taken into account. The respective values of α^q for Na^+, Ag^+, and Cl^- are 0.06, 1.15, and 9.73 Å^5.

VII. ENERGY TERMS

The energy E_d required to extract an ion or create an interstitial is given as a sum of various contributions:

$$E_d = W_{rl} + W_{\mathrm{Co}}^1 + W_{\mathrm{sr}}^1 + W_{\mathrm{sr}}^2 + W_{\mathrm{sr}}^{1,2} + W_p^1 + W_p^2 + W_q^1 \ , \tag{62}$$

where W_{rl} is the energy needed to create the defect assuming all the other ions are held fixed in their perfect lattice positions. W_{Co} is the Coulomb monopole interaction energy due to the presence of the virtual and real charges of region 1; $W_{\mathrm{sr}}^1 + W_{\mathrm{sr}}^2 + W_{\mathrm{sr}}^{1,2}$ is the change in the short range interactions amongst ions of region 1 as well as their first and second neighbors due to the relaxation of the first region; W_p^1 is the total dipolar polarization energy of region 1. This includes contribution from the interaction of region 2 dipoles with region 1 displacement dipoles in addition to the electronic part W_{pe}^1; W_p^2 is the second region polarization energy; and W_q^1 is the quadrupole polarization energy of region 1.

Two computer codes, one for the vacancy and one for the interstitial have been developed to estimate E_d. The computer programs are written to estimate the defect energies in the EPPI model. The code is general enough to accommodate any kind of potential model for the rock-salt structure. The simple but sound structure of the MPPI model and the symmetry of the induced quadrupole tensor have made it possible to simplify the computer code both in terms of time and computational efficiency. A number of checks have been carried out to ensure the correctness of the program.

The computer code for the interstitial defect involves solving four coupled linear equations to evaluate the induced dipole and quadrupole moments. These are solved for *exactly* using the symbolic MACSYMA software. As these quantities are to be evaluated for each of the mesh points in the domain of displacement variables s_c and s_a, this analytical method of solution minimizes errors in the computation as well as the time involved. A direct search method was used to locate the minimum of the total energy of the defect lattice. The enthalpies of formation of Schottky and Frenkel defects are then given by

$$h_S = W_{av} + W_{cv} - U_1 \ , \qquad h_F = W_{cv} - W_{\mathrm{int}} \ . \tag{63}$$

Here W_{av}, and W_{cv} are the energies (E_d) needed to extract an anion and cation, respectively, and W_{int} is the energy needed to accommodate an ion at the interstitial site. U_1 is the cohesive energy of the salt, estimated within the scheme of interionic potentials used in our calculation. The results are tabulated and discussed in detail in the next section.

VIII. RESULTS AND DISCUSSION

A. MPPI model

In order to highlight the essential difference between the two salts AgCl and NaCl, we give a comparison of

TABLE V. Cation interstitial—various energy contributions; $\alpha^q=0.0$ Å^5. (All energy terms in units of eV.)

Salt	$s_{c,a}$(min)	RLE	Coul	Rep	vdW	W_p^1	W_p^2	W_{int}
AgCl	s_c: 0.06 s_a: 0.02	1.84	−1.05	−1.68	1.39	−1.68	−1.77	−2.99
NaCl	s_c: 0.14 s_a: 0.00	2.07	−3.00	1.14	0.03	−0.20	−1.57	−1.68
NaCl*	s_c: 0.16 s_a: 0.00	2.98	−3.32	0.79	−0.04	−0.08	−1.57	−1.42

[a]Potential parameters from the Fumi-Tosi model (Ref. 16).

TABLE VI. AgCl cation vacancy; RLE=8.851 eV, $W_p^2=-1.84$ eV.

α_a^q (Å^5)	s_a	p_a (10^{-18} esu)	W_p^1 (eV)	Q^a (10^{-26} esu)	W_q^1 (eV)	W_{cv} (eV)
0.0	−0.005	−1.381	−1.68	0.00	0.00	5.41
6.50	−0.025	−1.393	−1.89	2.691	−0.652	4.94
5.53	−0.020	−1.380	−1.82	2.283	−0.540	5.01
9.73	−0.045	−1.452	−2.18	4.092	−1.089	4.69

TABLE VII. AgCl anion vacancy; RLE=9.15 eV, $W_p^2=-2.08$ eV.

α_c^q (Å^5)	s_c	p_c (10^{-18} esu)	W_p^1 (eV)	Q^c (10^{-26} esu)	W_q^1 (eV)	W_{av} (eV)
0.0	0.040	0.410	−0.28	0.00	0.00	6.33
2.62	0.020	0.445	−0.42	−1.101	−0.215	6.16
1.44	0.030	0.427	−0.35	−0.585	−0.109	6.23
1.153	0.035	0.416	−0.31	−0.457	−0.083	6.25

the various energy contributions in the three defect environments in Tables III–V. In these tables the energy terms RLE, Coul, Rep, and vdW correspond to the contribution of the rigid lattice energy, Coulomb, short-range repulsion, and van der Waals interactions to the defect formation. $s_{c,a}(\min)$ are the equilibrium values of displacement. These contributions are only dependent on the relaxation and not on the α^q's. The polarization terms are computed within the MPPI model.

From the above tables it can be seen that the equilibrium displacements of the region-1 ions are in general much smaller in AgCl than in NaCl for the vacancy defects. The first-region polarization energies (W_p^1) are relatively much larger in AgCl than in NaCl, as the dipole polarizabilities are larger in AgCl (see Table II). For the anion vacancy in NaCl the net polarization energy of region 1 turns positive owing to a larger depolarization associated with the displacement dipoles in the dipolar field of region 2.

In contrast to NaCl, the van der Waals forces in AgCl are stronger and provide a partial compensation to the effect of the repulsion forces. This feature is more pronounced in the case of the interstitial and is one of the important factors responsible for the dominance of Frenkel disorder in AgCl.

Tables III–V contain, in the third row, results for NaCl based on the Fumi-Tosi interionic potentials and other input data compatible with the MPPI model.[9] It may be seen that the defect energies are not radically modified compared to the results for the present poten-

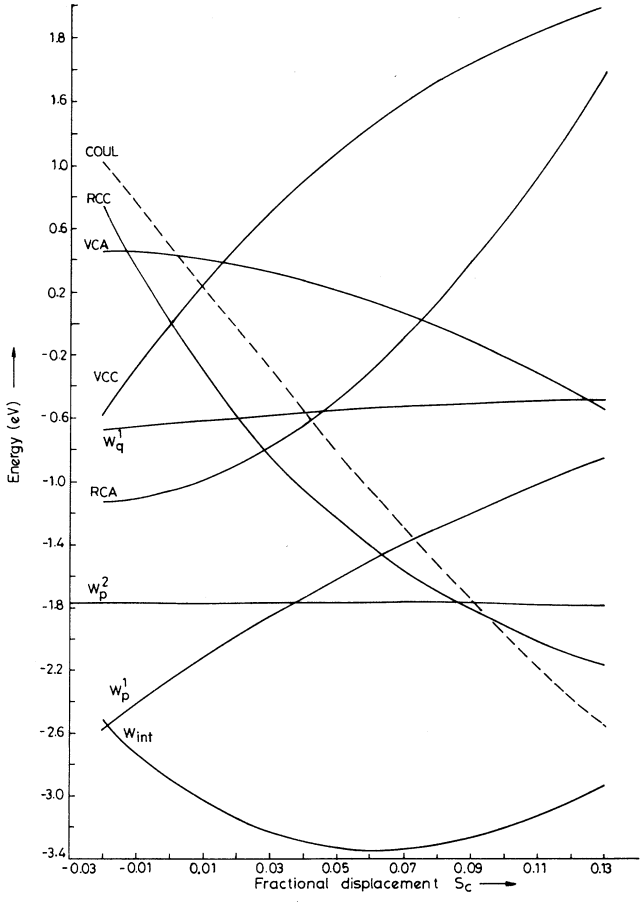

FIG. 2. Cation interstitial defect. Contributions of various energy terms are shown as a function of region-1 cation relaxation s_c for a fixed value of anion relaxation ($s_a=0.02$), in AgCl.

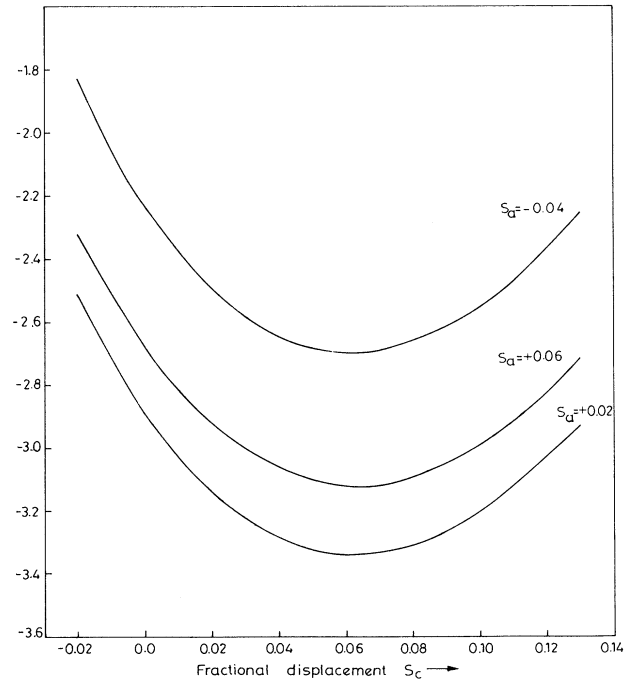

FIG. 3. Variation of interstitial formation energy (W_{int}) in AgCl as a function of the cation relaxation s_c for three different values of anion relaxation s_a.

TABLE VIII. AgCl cation interstitial; RLE=1.838 eV, $W_p^2=-1.77$ eV.

α^q (Å^5)	s_c	s_a	p_c (10^{-18} esu)	p_a (10^{-18} esu)	W_p^1 (eV)	Q^c (10^{-26} esu)	Q^a (10^{-26} esu)	W_q^1 (eV)	W_{int} (eV)
a: 0.0 c: 0.0	0.06	0.02	0.467	1.497	−1.678	0.00	0.00	0.00	−2.99
a: 6.50 c: 2.62	0.06	0.02	0.409	1.368	−1.517	−0.326	−1.420	−0.634	−3.46
a: 5.53 c: 1.44	0.06	0.02	0.414	1.404	−1.552	−0.184	−1.258	−0.524	−3.39
a: 9.73 c: 1.15	0.06	0.02	0.373	1.379	−1.490	−0.022	−2.168	−0.796	−3.60

tial, thus pointing to the relative insensitivity of the defect calculations to the details of the crystal potential.

B. EPPI model: AgCl

The results for the vacancy and interstitial defects in AgCl in the EPPI model are displayed in Tables VI–VIII. Column 1 of Table VI (VII) for the cation (anion) vacancy in AgCl corresponds to the four cases introduced in Sec. V. Since the region-1 ions are anions (cations), α_a^q, (α_c^q) is the quantity of interest. The second column of the table gives the value of the equilibrium displacement s_a (s_c). The corresponding values of the induced dipole moment p_a (p_c), the induced quadrupole moment Q^a (Q^c), and their contributions to the polarization energy are tabulated in columns 3–6.

In the case of the cation interstitial, since region 1 contains anions and cations, both Q^c and Q^a contribute. The minimum of the energy of formation of an interstitial is then a function of both s_c and s_a. The corresponding dipole and quadrupole moments and their contribution to energy are tabulated. In Table IX we give the formation enthalpies of Schottky and Frenkel defects for the four cases. The following comments are in order.

(1) The last row in each of the Tables VI–IX corresponds to the α^q of the free ions and, especially in the case of Cl^- ion, the values in this row must be taken as limiting values. In the following discussion the focus is then on values of α^q corresponding to cases 2 and 3.

(2) In AgCl, inclusion of quadrupoles is necessary. This can be seen from the fact that in the case of cation vacancy the contribution of the quadrupolar polarization energy is about 12% of the defect formation energy, while it is 3% in the case of anion vacancy and 15% for the interstitial.

(3) The larger values of the anion quadrupole moments, reflected in the larger contribution of the quadrupoles to the cation vacancy and the interstitial defect formation, show that Cl^- is more deformable. The quadrupolar moment is a direct measure of the departure from the sphericity of the ion in the presence of the defect. The Ag^+ quadrupole contributes marginally to the defect enthalpy, and so the silver ion is seen more in the role of a polarizer rather than as being polarizable. This inference is supported by the fact that while the Ag^+ ions displace considerably from their lattice positions, the Cl^- ions are not easily displaced. That the Cl^- ion is more polarizable and deformable in AgCl is borne out by other investigations.[32,36]

(4) Inclusion of quadrupolar deformation enhances the dipole polarization energy in the case of the cation vacancy but decreases it for the interstitial. With the positive sign of the anion quadrupole moment (Q^a) around the cation vacancy, the anion dipole moment p_a is enhanced as a result of the extra field contributed by Q^a. The sign of Q^a for the anions around the cation interstitial is negative and hence reduces the induced dipole moments.

(5) In the case of a vacancy defect, the inclusion of the quadrupoles shifts the equilibrium displacement inwards, in contrast to the interstitial case. The overall first-region polarization energy (W_p^1 and W_q^1) generally favors inward displacement. The increase in the magnitude of this energy, upon the inclusion of quadrupoles, is relatively much larger in the case of a vacancy (see the preceding comment) than for the interstitial.

(6) Figure 2 depicts the variation of individual energy terms with s_c for the equilibrium value of s_a in the case of the interstitial defect. It may be seen that the Coulomb term (COUL) strongly favors outward displacement of the cations while the first-region polarization energy

TABLE IX. AgCl point defect formation enthalpies; $U_1=9.01$ eV. All values are in eV.

α^q	W_{cv}	W_{av}	W_{int}	h_S	h_F
Case 1	5.41	6.33	−2.99	2.73	2.42
Case 2	4.94	6.16	−3.46	2.09	1.48
Case 3	5.01	6.23	−3.39	2.23	1.62
Case 4	4.69	6.25	−3.60	1.93	1.09

TABLE X. NaCl cation vacancy; RLE=8.02 eV, $W_p^2=-1.70$ eV.

$\alpha_{a^5)}^q$ (Å)	s_a	p_a (10^{-18} esu)	W_p^1 (eV)	Q^a (10^{-26} esu)	W_q^1 (eV)	W_{cv} (eV)
0.0	0.080	−0.302	−0.06	0.00	0.00	5.20
5.33	0.070	−0.305	−0.09	1.560	−0.225	5.00
5.53	0.060	−0.322	−0.14	1.700	−0.255	4.99
9.73	0.050	−0.326	−0.18	3.008	−0.474	4.83

TABLE XI. NaCl anion vacancy; RLE=8.00 eV, $W_p^2=-1.79$ eV.

α_c^q (Å^5)	s_c	p_c (10^{-18} esu)	W_p^1 (eV)	Q^c (10^{-26} esu)	W_q^1 (eV)	W_{av} (eV)
0.0	0.090	0.041	0.21	0.00	0.00	5.29
0.06	0.085	0.043	0.20	0.017	−0.002	5.29

(W_p^1) would favor an inward displacement. We further note that the magnitude of the short-range repulsion energy is large because the ions are in a volume one-eighth of the volume for the vacancy. RCA and VCA are the overlap repulsion and van der Waals interaction energies of region-1 cations and anions with their nearest neighbors. For a given value of s_a, the contributions to these terms from the interactions between the interstitial and other nearest-neighbor anions are not dependent on s_c. However, the repulsion (RCC) and van der Waals (VCC) interactions among cations includes a large contribution from the real ion at the defect site. This results in a detailed balance of attractive and repulsive short-range forces. The overall minimum of the energy function $W_{\text{int}}(s_c,s_a)$ is located by a direct search procedure. Figure 3 shows the variation with s_c for three values of s_a about the global minimum.

C. EPPI: NaCl

In Tables X–XIII we present the results for the NaCl within both the MPPI ($\alpha^q=0$) and EPPI models. For Na^+ the values of α^q in cases 2, 3, and 4 are nearly the same and so for the anion vacancy only two cases, i.e., with and without the quadrupoles, are considered.

The small quadrupole polarizability of the Na^+ ion, as might be expected, results in a marginal value of W_q^1 in the case of the anion vacancy. However, in the case of the cation vacancy and cation interstitial, the quadrupole polarization energy is surprisingly larger than the dipole contribution. We believe that this is an indication that the value of α_q used for Cl^- in NaCl is unduly large. It may be recalled (Sec. III) that the dipolar polarizability has been modeled in our scheme as a crystal-dependent property in order to account for the effects of short-range polarizations leading to different values for $\alpha_{c,a}$ in AgCl and NaCl (see Table II). It appears necessary to incorporate such an effect in the determination of the appropriate α^q for each crystal.

IX. CONCLUSIONS

In the foregoing pages, we have presented a detailed formulation of the EPPI model for the vacancy and interstitial defects in an ionic crystal. The model offers a simple, physically sound, and computationally efficient technique of simulating point defects in ionic solids. The output of the simulation comprises, besides the defect enthalpies, the center of mass displacements, dipole moments, and quadrupole moments—all physically significant measures of the distorted polarized lattice.

The model has been applied to Schottky defects and Frenkel defects in AgCl and NaCl. A major finding of the work is that any simulation of charged point defects in ionic crystals should include effects of multipolar deformations. This follows from the fact the induced quadrupoles not only provide an extra and substantial contribution to the polarization energy but also affect the dipolar energy term. We get, for AgCl, formation enthalpies of Schottky defects (2.09 eV) and Frenkel defects (1.48 eV) in reasonable agreement with currently available experimental findings, but only upon inclusion of the quadrupolar deformations.

In the case of NaCl, the effects are unduly large and contrary to expectations. We consider this to be the result of using an overestimated α^q for Cl^- in the crystal environment. It appears desirable to determine the quadrupolar polarizabilities by matching with a suitable macroscopic response such as dielectric or elastic properties of the crystal.

We would like to point out that the EPPI model presented here does not suffer from any arbitrariness and provides a natural physical approach based on the electrostatics of the problem. To cite an example, in previous models[29,30] the estimation of both h_S and h_F, in agreement with experiments in AgCl, warranted refinements of

TABLE XII. NaCl cation interstitial; RLE=2.077 eV, $W_p^2=-1.57$ eV.

α^q (Å^5)	s_c	s_a	p_c (10^{-18} esu)	p_a (10^{-18} esu)	W_p^1 (eV)	Q^c (10^{-26} esu)	Q^a (10^{-26} esu)	W_q^1 (eV)	W_{int} (eV)
a: 0.0 *c*: 0.0	0.14	0.00	0.056	0.411	−0.206	0.00	0.00	0.00	−1.68
a: 5.33 *c*: 0.06	0.13	−0.02	0.047	0.403	−0.210	−0.001	−1.359	−0.463	−2.09
a: 5.53 *c*: 0.06	0.13	−0.02	0.047	0.402	−0.209	0.001	−1.406	−0.479	−2.10
a: 9.73 *c*: 0.06	0.12	−0.02	0.046	0.398	−0.226	0.022	−2.378	−0.817	−2.41

TABLE XIII. NaCl point defect formation enthalpies; $U_1 = 8.01$ eV. All values are in eV.

α^q	W_{cv}	W_{av}	W_{int}	h_S	h_F
Case 1	5.20	5.29	−1.68	2.48	3.52
Case 2	5.00	5.29	−2.09	2.28	2.91
Case 3	4.99	5.29	−2.10	2.27	2.89
Case 4	4.83	5.29	−2.41	2.11	2.42

the potential such as adding three-body interactions. We, however, find that within a two-body central force potential which represents the broad features of the interionic interactions, the EPPI model gives a good estimate of both h_S and h_F. The model is also able to predict the dominant defect species in both AgCl and NaCl, within the same polarization and potential scheme.

These results further suggest that the quadrupolar deformations (especially of the anions) may have a salient role to play in the migration processes. These are under study.

ACKNOWLEDGMENTS

We wish to thank the Institute of Mathematical Sciences for making available the MACSYMA software. R.D.B. acknowledges the CSIR, India for financial support. We are thankful to Professor K. V. S. Rama Rao for providing encouragement and general support.

[1]R. J. Friauf, J. Phys. (Paris) Colloq. **41**, C6-97 (1980).
[2]A. L. Laskar, in *Superionic Solids and Solid Electrolytes,* edited by A. L. Laskar and S. Chandra (Academic, London, 1989), p. 265.
[3]A. R. Allnatt, P. Pantelis, and S. J. Sime, J. Phys. C **4**, 1778 (1971).
[4]F. Beniere, M. Beniere, and M. Chemla, J. Phys. Chem. Solids **31**, 1205 (1970).
[5]N. F. Mott and M. J. Littleton, Trans. Faraday Soc. **34**, 485 (1938).
[6]B. G. Dick and A. W. Overhauser, Phys. Rev. **112**, 90 (1958).
[7]J. R. Hardy and A. M. Karo, *The Lattice Dynamics and Statics of Alkali Halide Crystals* (Plenum, New York, 1979), p. 60.
[8]P. W. M. Jacobs, J. Corish, and C. R. A. Catlow, J. Phys. C **13**, 1977 (1980).
[9]Y. V. G. S. Murti and V. Usha, Physica **83B**, 275 (1976).
[10]R. A. Cowley *et al.*, Phys. Rev. **131**, 1030 (1963).
[11]R. D. Banhatti and Y. V. G. S. Murti, Phys. Status Solidi B **166**, 15 (1991).
[12]W. Jost, J. Chem. Phys. **1**, 466 (1933).
[13]M. J. Norgett (unpublished).
[14]J. R. Tessmann, A. H. Kahn, and W. Shockley, Phys. Rev. **92**, 890 (1953).
[15]B. Szigeti, Proc. R. Soc. London, Ser. A **204**, 51 (1950).
[16]M. P. Tosi, in *Solid State Physics,* edited by F. Seitz and D. Turnbull (Academic, New York, 1964), Vol. 16, p. 1.
[17]I. D. Faux and A. B. Lidiard, Z. Naturforsch. Teil A **26**, 62 (1971).
[18]Y. V. G. S. Murti and R. D. Banhatti, in *Proceedings of the International Conference on Defects in Insulating Materials,* 1992, edited by O. Kanert and J.-M. Spaeth (World Scientific, Singapore, 1993).
[19]A. Dalgarno, Adv. Phys. **11**, 281 (1962).
[20]A. D. Buckhingham, in *Intermolecular Forces,* edited by J. O. Hirschfelder (Interscience, New York, 1967).
[21]The corresponding expression in Ref. 11 is erroneous. Also, it was based on a preliminary formulation of the EPPI model.
[22]R. G. Gordon and Y. S. Kim, J. Chem. Phys. **56**, 3122 (1972).
[23]Y. S. Kim and R. G. Gordon, J. Chem. Phys. **60**, 4332 (1974).
[24]C. R. A. Catlow, J. Corish, and P. W. M. Jacobs, J. Phys. C **12**, 3433 (1979).
[25]M. Bucher, Phys. Rev. B **30**, 947 (1984).
[26]R. D. Banhatti, Y. V. G. S. Murti, and A. L. Laskar, Phys. Status Solidi B **164**, 357 (1991).
[27]C. E. Moore, *Atomic Energy Levels,* National Standard Reference Data System Vol. III (U.S. GPO, Washington, D.C., 1971), p. 35.
[28]H. Hotop and W. C. Lineberger, J. Phys. Chem. Ref. Data **4**, 539 (1975).
[29]F. Granzer *et al.*, J. Phys. (Paris) Colloq. **41**, C6-101 (1980).
[30]R. C. Baetzold *et al.*, J. Phys. Chem. Solids **50**, 791 (1989).
[31]R. P. Lowndes and D. H. Martin, Proc. R. Soc. London, Ser. A **308**, 473 (1969).
[32]H. Takahashi, S. Tamaki, and Y. Waseda, Solid State Ionics **31**, 55 (1988).
[33]G. D. Mahan, Phys. Rev. A **22**, 1780 (1980).
[34]G. D. Mahan, Phys. Rev. B **34**, 4235 (1986); **38**, 7841 (1988).
[35]P. C. Schmidt, A. Weiss, and T. P. Das, Phys. Rev. B **19**, 5525 (1979).
[36]G. D. Mahan and Mark Mostoller, Phys. Rev. B **34**, 5726 (1986).